

*Citation for published version:*

Kim, J-H, Resende, R, Wennekes, T, Chen, H-M, Bance, N, Buchini, S, Watts, AG, Pilling, P, Streltsov, VA, Petric, M, Liggins, R, Barrett, S, Mckimm-Breschkin, JL, Niikura, M & Withers, SG 2013, 'Mechanism-based covalent neuraminidase inhibitors with broad spectrum influenza antiviral activity', *Science*, vol. 340, no. 6128, pp. 71-75. <https://doi.org/10.1126/science.1232552>

DOI:

[10.1126/science.1232552](https://doi.org/10.1126/science.1232552)

Publication date:

2013

Document Version

Peer reviewed version

[Link to publication](#)

This is the author's version of the work. It is posted here by permission of the AAAS for personal use, not for redistribution. The definitive version was published in *Science*, vol 340, 5th April 2013, DOI: [10.1126/science.1232552](https://doi.org/10.1126/science.1232552)

University of Bath

General rights

Copyright and moral rights for the publications made accessible in the public portal are retained by the authors and/or other copyright owners and it is a condition of accessing publications that users recognise and abide by the legal requirements associated with these rights.

Take down policy

If you believe that this document breaches copyright please contact us providing details, and we will remove access to the work immediately and investigate your claim.

Title: Mechanism-based Covalent Neuraminidase Inhibitors with Broad Spectrum Influenza Antiviral Activity

Authors: Jin-Hyo Kim^{1,†,*}, Ricardo Resende^{1,*}, Tom Wennekes^{1,‡,*}, Hong-Ming Chen^{1,*}, Nicole Bance², Sabrina Buchini¹, Andrew G. Watts³, Pat Pilling⁴, Victor A. Streltsov⁴, Martin Petric⁵, Richard Liggins⁶, Susan Barrett⁴, Jennifer L. McKimm-Breschkin⁴, Masahiro Niikura² and Stephen G. Withers^{1*}

Affiliations:

¹Department of Chemistry, University of British Columbia, 2036 Main Mall, Vancouver, B.C., V6T1Z1, Canada.

²Faculty of Health Sciences, Simon Fraser University, 8888 University Drive, Burnaby, B.C., V5A1S6, Canada.

³Department of Pharmacy and Pharmacology, University of Bath, Claverton Down, Bath, BA27AY, UK.

⁴CSIRO Materials Science and Engineering, 343 Royal Pde, Parkville, 3052, Australia.

⁵British Columbia Centre for Disease Control, Provincial Health Services Authority, Vancouver, BC, V5Z 4R4, Canada.

⁶Centre for Drug Research and Development (CDRD), 2259 Lower Mall, Vancouver, B.C., V6T 1Z4, Canada.

*These authors contributed equally.

†Current address: Division of Chemical Safety, National Academy of Agricultural Science, RDA, 126 Suin-ro, Suwon, 441-707, Republic of Korea.

‡Current address: Laboratory of Organic Chemistry, Wageningen University, Dreijenplein 8, 6703 HB Wageningen, The Netherlands.

*Correspondence to: withers@chem.ubc.ca.

One Sentence Summary: Specific, covalent, mechanism-based inhibitors of influenza neuraminidase function as potent ($IC_{50} = 1 - 10$ nM) antiviral agents *in vitro* and protect mice against infection.

Abstract: Influenza antiviral agents play important roles in modulating disease severity and in controlling pandemics while vaccines are prepared, but the development of resistance to agents like the commonly used neuraminidase inhibitor Tamiflu may limit their future utility. We report here a completely new class of specific, mechanism-based anti-influenza drugs that function via the formation of a highly stabilized covalent intermediate in the neuraminidase enzyme, and confirm this mode of action via structural and mechanistic studies. These compounds function not only in cell-based assays, but also in animal models, with efficacies comparable to that of Relenza and with broad spectrum activity against drug-resistant strains *in vitro*. With their great structural similarity to the natural substrate, and their novel mode of action based upon the enzyme mechanism, this class of drug should be less prone to resistance development, offering a new approach to the control of influenza.

Main Text:

The envelope of the influenza virus contains two immunodominant glycoproteins, hemagglutinin (HA) and neuraminidase (NA), that play key roles in viral infection and spread. HA effects attachment of the virus to the host cell via its interaction with surface sialic acids, thereby initiating entry. Once the virus has replicated, the NA cleaves sialic acids from the viral and cell surfaces, allowing the virus progeny to spread to uninfected cells. The specific antigenic properties of the different HAs and NAs are used to classify influenza type A viruses into subtypes (H1-17 and N1-9). These in turn can be categorized into two groups on the basis of neuraminidase phylogeny: Group 1 contains N1, N4, N5 and N8, while Group 2 contains N2, N3, N6, N7 and N9. Based on the notion that potent and specific viral NA inhibitors should function to reduce viral spread, structure-based inhibitor design programs have produced two widely used anti-influenza drugs, zanamivir (Relenza[®]) and oseltamivir (Tamiflu[®]) (Fig. 1A). Oseltamivir figured prominently in the control of the recent H1N1 pandemic. The initial design of these drugs was based upon the mimicry of the flattened transition state conformation of the sugar through incorporation of an endocyclic alkene within a carbocycle (oseltamivir) or a pyranose ring (zanamivir) (1). Specificity for the influenza enzyme over other neuraminidases, along with additional affinity, was provided by incorporation of a guanidinium or ammonium substituent at the position corresponding to C-4 of the natural substrate to interact with a highly

conserved anionic pocket at that location in the active site. These broad spectrum influenza drugs are active against NAs from group 1 and 2 influenza A strains as well as influenza B.

We are now seeing the emergence of drug-resistant strains, particularly against the more widely used and structurally divergent drug oseltamivir. Mutations can be both drug- and influenza subtype- specific. The most commonly seen mutation in viruses with the N1 subtype is H275Y which interferes with binding of the isopentyl side chain of oseltamivir, but still permits binding of zanamivir and the natural substrate. Mutations most commonly detected in clinical isolates with the N2 subtype include R292K (2-4) and E119V (3, 4). Like the H275Y, the R292K precludes full rotation of the E276 necessary to create the hydrophobic pocket that accommodates the pentyl side-chain of oseltamivir (5). In contrast, E119V confers oseltamivir specific resistance due to altered interactions with the 4-amino group. E119A,D,G mutations seen *in vitro* (6, 7) affect binding of oseltamivir and/or zanamivir, demonstrating the critical nature of the interactions of C-4 amino or guanidino group for high affinity binding. Some of the recent mutations seen in pandemic H1N1 viruses, including I223R, confer reduced sensitivity to both inhibitors (8-10). The emergence of these mutant strains highlights an urgent need for new classes of NA inhibitors that differ minimally in structure from the parent sialic acid, given that the development of resistance to structurally conservative, mechanism-based inhibitors should be a much less probable event (5).

Diffluorosialic acids are covalent NA inhibitors that react with Y406 as the catalytic nucleophile

NAs catalyze the hydrolysis of sialosides by a process resulting in net retention of stereochemistry at the site of substitution. A mechanism involving an ion-pair intermediate has long been suggested for the GH34 (11) influenza NA (12), though involvement of a covalent intermediate, as has been shown for GH33 NAs (13), has emerged as an alternative. We here provide the first evidence for a covalent intermediate formed in the course of the reaction catalyzed by the influenza NA by use of 2,3-difluorosialic acid (**1**, DFSA) (Fig. 1B) as a substrate that exhibits slow turnover. The electronegative fluorine atom at C-3 inductively destabilizes the oxocarbenium ion-like transition states for both formation and hydrolysis of the intermediate, thus slowing each step, while the C-2 anomeric fluoride leaving group speeds the formation step, permitting accumulation of the covalent intermediate (Fig. 1B). Rapid

inactivation of NA was observed at low inactivator concentrations, such that individual kinetic parameters (K_i and k_i) could not be determined for the N9 NA; only a second order rate constant k_i / K_i of $196 \text{ min}^{-1} \text{ mM}^{-1}$ could be measured. Turnover of the covalent intermediate (k_{hydr}) also occurred rapidly, with a $t_{1/2} < 1$ minute. Confirmation of the formation of a covalent species and identification of the site of attachment was achieved by peptic digestion of N9 NA that had been labeled with 2,3-difluorosialic acid **1**, or by its difluoroKDN analogue as shown in fig. S1-3. Isolation and subsequent sequence analysis of the labeled peptide by LC/MS-MS identified this peptide as NTDWSGYSSSGSF, with the tyrosine (Y) bearing the sugar label. This provides direct evidence for a role of Y406 as the catalytic nucleophile.

With the knowledge that the influenza NAs employ a covalent mechanism, we embarked on a program to explore these 2,3-difluoro sialic acids (DFSAs) as a possible new class of mechanism-based influenza therapeutics that inhibit by covalently blocking the active site. This is an attractive approach since not only can the initial affinity of the drug (K_i) be optimized, but also, the relative rate constants for formation (k_i) and hydrolysis (k_{hydr}) of the trapped intermediate, with the objective being to optimize the ratio of k_i/k_{hydr} . Such a strategy has worked well previously for the β -lactam antibiotics, and may provide particularly favorable pharmacokinetic behavior in this situation. Indeed covalent drugs are regaining respect, with three of the top-selling drugs in the U.S. being covalent inhibitors of their targets (14). Key improvements required to convert **1** into a useful drug candidate are therefore to introduce selectivity for the viral NA over host enzymes and to drastically reduce rates of turnover (k_{hydr}). Since the incorporation of an equatorial cationic nitrogen substituent at the site equivalent to OH-4 of sialic acid provided a substantial affinity boost within zanamivir and oseltamivir, it was of interest to synthesize versions of **1** bearing amine (Am) and guanidine (Gu) substituents at C-4. Not only might these electron-withdrawing substituents improve the initial affinity and the specificity for the influenza enzyme, but also turnover of the intermediate may be further slowed, due both to the additional stabilization of the bound intermediate provided through improved interactions with the enzyme, and to the added inductive effect of the substituent on the reaction transition state. The effects of axial (ax) or equatorial (eq) stereochemistry of F3 on inhibitory behavior were also explored.

Synthesis of the protected diastereomeric 3-axial and 3-equatorial-2,3-difluoro-4-azido neuraminic acids as key intermediates was achieved by Selectfluor™ hydroxyfluorination of 2,4-dideoxy-2,3-didehydro-4-azido-N-acetylneuraminic acid (4-azido-DANA) (15) followed by installation of an equatorial fluorine at C-2 using diethylaminosulfur trifluoride (DAST). The lead candidates shown in Table 1, FaxAmDFSA (2), FaxGuDFSA (3), FeqAmDFSA (4) and FeqGuDFSA (5) were then prepared by reduction or reductive guanidylation, followed by deprotection. Full synthetic details and product characterization are provided as Supplementary Materials.

Selective inhibition of influenza virus NA *in vitro*

Kinetic parameters for inactivation and reactivation of N1, N2 and N9 NAs, as representatives of the Group 1 and Group 2 enzymes, by 2 - 5 are presented in Tables 1 and S4, along with parameters for the parent 2,3-difluorosialic acid 1 with the N9 NA. As noted, inactivation by 1 was too fast, even at 4 °C, for individual parameters of the inactivation rate (k_i) and binding (K_i) constants to be measured, thus only the second order rate constant (k_i/K_i) was determined. Rate constants for turnover by hydrolysis (k_{hydr}) were determined by monitoring the time course of reactivation of dialyzed, inactivated enzyme, and fitting the data to a first order expression. First order rate constants for inactivation and reactivation are also expressed in the form of half-lives for each process in Table 1.

Gratifyingly, not only does incorporation of the charged substituent at C-4 result in high initial affinity, but also, more importantly, it greatly reduces the rate constant for reactivation of enzymes inactivated by 2, 3, 4 and 5. Half-lives for reactivation of NAs labeled by 2, 3, 4 and 5 ranged from 0.75 h to >100 h. These very slow turnover rates are extremely important as they mean that the virus will remain inactivated for extended times, even after the compound may have been cleared from relevant tissues, with favorable consequences for pharmacokinetic behavior. Interestingly, compounds with an equatorial fluorine at C-3 inactivate and reactivate faster than do those with an axial fluorine, typically by 10-40 fold. Further, the presence of a guanidine substituent at C-4 slows both the inactivation and reactivation more than does an amine substituent, with a much greater effect on the reactivation step. Since the two transition states (for formation and hydrolysis) will be very similar, this difference in rate likely has its origins in optimized interactions of the guanidine with the active site at the stage of the covalent

intermediate, as is seen in the crystal structure of the trapped species shown in Fig. 1C. A covalent bond of 1.45 Å is clearly observed in the electron density map (Fig. 1C, table S1), between C-2 of 3-fluoro (eq) sialic acid and the phenolic oxygen of Y406. As observed previously in a structure of the GH33 sialidase NanI (16), the covalent intermediate species is accompanied by an unsaturated form of fluorosialic acid formed by elimination. The carboxylate groups of both bound species form electrostatic interactions with the guanidine groups of the strictly conserved arginine triad R118, R292 and R371, a key interaction common among existing NA inhibitors. However, the elimination product forms stronger interactions (≤ 3 Å) with R118 and R371 (fig. S4) similar to those formed with zanamivir, while the covalent intermediate exhibits shorter contacts (≤ 3 Å) with R292 (Fig. 1D). In addition to many other interactions that have been observed in previous complexes of N9 NA with zanamivir (17), both forms of FeqGuDFSA also form electrostatic interactions at 2.9-3.4 Å (Fig. 1D and fig. S4) between the equatorial fluorine and the positive charge of the guanidine group of R118, reminiscent of those seen in other protein/ligand systems (18), possibly explaining the higher initial affinity of the FeqGuDFSA (5) inhibitor compared to others. The C-4 guanidine indeed forms strong interactions with the anionic pocket, very similar to those found with zanamivir (1), thereby contributing to stabilization of the intermediate.

An absolute comparison of the *in vitro* efficacy of these compounds as enzyme inhibitors with those of zanamivir or oseltamivir is difficult and not necessarily instructive given their different modes of action, covalent versus non-covalent and the time-dependence of inhibition: quite different results are obtained at different assay intervals (19). However, a pragmatic measure was achieved by measuring IC₅₀ values for each DFSA, as well as zanamivir and oseltamivir carboxylate (oseltamivir from which the pro-drug ester had been hydrolyzed), against four different virus strains after pre-incubation for 30 minutes prior to substrate addition. The IC₅₀ values so obtained are presented in Table 2, along with data for mutant viruses to be discussed below. Comparison between pairs of DFSAs again confirms that, in almost all cases, each compound with an equatorial fluorine is a superior inhibitor to its epimer with an axial fluorine, indicating that, under these conditions, improved rates of inactivation are important. Likewise, in each case the guanidine derivative showed superior performance to its amine analogue. Consequently, compound 5 (FeqGuDFSA) was the optimal derivative within the series. Comparison of these IC₅₀ values with those for zanamivir and oseltamivir reveals that, on

this measure, the compounds with an equatorial fluorine are of comparable efficacy, particularly when the guanidine is present. Further, their “on-rates” are superior to those of zanamivir, while off-rates are enormously slower (1, 20, 21).

The *specificity* of these inhibitors was then evaluated by testing them against Neu2 as a representative human NA (all human NAs belong to the sequence-related family GH33). No inactivation of Neu2 was seen with either of the amine derivatives, and inactivation by FaxGuDFSA (3) and FeqGuDFSA (5) occurred slowly, but at rates some $10^5 - 10^6$ lower than seen for inactivation of NA at comparable concentrations. This behavior is a considerable improvement over zanamivir, which inhibits Neu2 with a K_i of 17 μM , only $10^3 - 10^4$ fold higher than for NA (22).

Effects on influenza virus replication

Based upon these very promising results the ability of compounds 2 - 5 to inhibit the replication of the virus in cell culture was explored using MDCK cells. Three A strains (N1, N2 and N9) plus one B strain were tested in plaque size reduction assays (PRA), with zanamivir used as a control. While absolute sensitivity in the PRA depends on both the affinity of the HA for cell receptors as well as the NA function (23, 24), it is a useful assay for determining relative sensitivity to inhibitors. The PRA data showed that all DFSAs inhibited virus replication (Table 3, figs. S5-S8) with no cytotoxicity observed even at 5 mM DFSA concentrations, as measured by neutral red staining of viable cells. The H3N2 virus was less susceptible to all inhibitors compared to the other strains (fig. S7), due to the lower affinity of its HA, which allows viral spread with less NA activity (25). However, for all strains, substitution with the 4-amino group enhanced inhibition over the parent DFSA, and the 4-guanidino substitution further enhanced inhibition of virus replication. It is interesting that the stereochemistry of the fluorine substituent had little effect on efficacy for the compounds with a 4-amino substituent, apart from possibly a small enhancement with the B virus. However the presence of an equatorial fluorine in the 4-guanidino version resulted in a further 10-fold enhancement in potency for three strains tested, the one exception being G70C (H1N9), which was particularly well inhibited by the axial version also (fig. S8). Consequently, FeqGuDFSA (5) had the highest potency of all of the inhibitors, including zanamivir, against the influenza B virus (fig. S5) and performed comparably against the influenza A strains. Two points are particularly noteworthy at this stage. One is that

this behavior in PRA largely mirrors the *in vitro* kinetic data, with the compounds possessing an equatorial fluorine being superior to those with an axial fluorine, and the 4-guanidino substitution being superior to a 4-amino. The other is that the absolute IC₅₀ values in these PRAs are consistently lower than those for enzyme inhibition for all except FeqAmDFSA (**4**) and impressively in all cases are in the low nanomolar range. The relatively poor PRA data observed with FeqAmDFSA (**4**) likely reflects the faster reactivation of NA inactivated by this compound.

Efficacy against resistant strains. The DFSA derivatives proved effective *in vitro* against a series of resistant strains, with the FeqGuDFSA (**5**) again proving to be the most widely active (Table 2). All compounds proved effective against virus with the H275Y mutation that affects binding of the isopentyl side chain of oseltamivir, as might be predicted. This is also reflected in the very similar kinetic data measured for each DFSA derivative with another H275Y oseltamivir resistant strain and its parent (Table 1). While the E119G mutation, which affects interactions with the inhibitor's guanidine (**5**), led to a 20-fold reduction in efficacy of FaxGuDFSA, this was much less severe than the 250-fold reduction in zanamivir binding. The effectiveness of the FeqGuDFSA is particularly noteworthy, and highlights the different resistance profiles and modes of action of the DFSAs and zanamivir. Clearly, selection against transition state analogue binding (zanamivir) does not suppress covalent intermediate formation. Indeed in the case of the E119 mutations that target the 4-position, FeqGuDFSA (**5**) actually performed 10-fold better against the mutant strains than against the wild type. This most likely reflects slower reactivation of the trapped intermediate formed on the mutant, due to disruption of transition state-stabilizing interactions. This excellent profile against otherwise resistant strains is extremely promising and supports the concept of mechanism-based inhibition as a means to minimize selection of resistant strains.

***In vivo* efficacy studies.**

Prior to *in vivo* efficacy studies in mouse models, the pharmacokinetic properties of FaxGuDFSA (**3**) as a representative DFSA derivative were evaluated for administration by intravenous and intranasal routes, and compared with data collected in parallel for zanamivir. Levels of **3** in blood, lung and trachea were measured and half-lives determined. Intranasal dosing resulted in 92% bioavailability compared to that seen with intravenous injection, along with approximately

seven times higher peak concentrations (C_{\max}) and ten times higher total exposure ($AUC_{(0-120 \text{ min})}$) in both lung and trachea compared to the intravenous route. Further, the plasma half-life of FaxGuDFSA (**3**) was also significantly longer after intranasal administration than after IV injection (table S2). The general similarity of this pharmacokinetic behavior to that of zanamivir, consistent with the similar polarities of the two compounds, encouraged us to test the efficacy via intranasal administration, using zanamivir as our control.

Efficacy tests were conducted using a mouse-adapted influenza A virus strain, A/Hong Kong/1/68 (H3N2) (26). Balb/c mice were treated with either DFSA derivative, zanamivir or saline twice daily by intranasal administration, starting two hours prior to infection. Body weights and general condition were monitored and when the animals lost 20% body weight they were euthanized and scored as non-survivors. In an initial study using 1 mg/kg/day of DFSA derivatives FaxGuDFSA showed superior results to FaxAmDFSA in prolonging the survival of animals. When FaxGuDFSA was tested at a higher dose of 10 mg/kg/day it protected all the mice from the lethal infection, as did zanamivir (Fig. 2A). In order to confirm that the compounds were acting as anti-viral agents, the viral RNA loads in lung tissue were measured by qPCR. These results confirmed that survival was indeed associated with suppression of viral replication, in a similar manner to the effect of zanamivir.

Dose-dependency of FaxGuDFSA in the protection of mice was demonstrated with 100% efficacy at 10 mg/kg/day and less protection at lower doses (Fig. 2B and table S3). The compounds induced no ill-effect in the treated animals during the experiments compared to the saline control.

Conclusions

The DFSAs represent a novel class of potent, mechanism-based, specific NA inhibitor functioning by transient formation of a covalent intermediate species. Their high efficacy as enzyme inhibitors is matched by excellent anti-viral activity in cell-based plaque size reduction assays, at levels similar or superior to those for zanamivir. Furthermore, they show good inhibition of NAs from zanamivir or oseltamivir-resistant influenza virus strains, indicating an altered resistance profile. Most importantly, they function well in controlling influenza infections in an animal model, at levels comparable to those used for zanamivir. The similarity of their structure to that of the natural substrate and their mechanism-based design should decrease the

selection of resistant viral strains, improving the therapeutically useful `lifetime` of this drug class.

References and Notes:

1. M. von Itzstein *et al.*, *Nature* **363**, 418 (1993).
2. J. L. McKimm-Breschkin *et al.*, *J. Virol.* **72**, 2456 (1998).
3. M. Tashiro *et al.*, *Antivir. Ther.* **14**, 751 (2009).
4. M. Kiso *et al.*, *Lancet* **364**, 759 (2004).
5. J. N. Varghese *et al.*, *Structure* **6**, 735 (1998).
6. T. J. Blick *et al.*, *Virology* **214**, 475 (1995).
7. L. V. Gubareva, M. J. Robinson, R. C. Bethell, R. G. Webster, *J. Virol.* **71**, 3385 (1997).
8. A. Eshaghi *et al.*, *Emerg. Infect. Dis.* **17**, 1472 (2011).
9. H. T. Nguyen, A. M. Fry, P. A. Loveless, A. I. Klimov, L. V. Gubareva, *Clin. Infect. Dis.* **51**, 983 (2010).
10. E. van der Vries, F. F. Stelma, C. A. Boucher, *N. Engl. J. Med.* **363**, 1381 (2010).
11. The CAZY Glycoside Hydrolase (GH) database classifies carbohydrate-active enzymes on the basis of sequence similarities. Most bacterial and mammalian sialidases/neuraminidases belong to family GH33.
12. M. von Itzstein, *Nat. Rev. Drug Discov.* **6**, 967 (2007).
13. A. G. Watts *et al.*, *J. Am. Chem. Soc.* **125**, 7532 (2003).
14. J. Singh, R. C. Petter, T. A. Baillie, A. Whitty, *Nature Rev. Drug Discov.* **10**, 307 (2011).
15. M. von Itzstein, B. Jin, W. Y. Wu, M. Chandler, *Carbohydr. Res.* **244**, 181 (1993).
16. S. L. Newstead *et al.*, *J. Biol. Chem.* **283**, 9080 (2008).
17. J. N. Varghese, V. C. Epa, P. M. Colman, *Protein Sci.* **4**, 1081 (1995).
18. J. A. K. Howard, V. J. Hoy, D. O'Hagan, G. T. Smith, *Tetrahedron* **52**, 12613 (1996).
19. S. Barrett, P. G. Mohr, P. M. Schmidt, J. L. McKimm-Breschkin, *PLoS One* **6**, e23627 (2011).
20. P. J. Collins *et al.*, *Nature* **453**, 1258 (2008).
21. E. van der Vries *et al.*, *PLoS Pathog.* **9**, (2012).
22. L. M. Chavas *et al.*, *J. Med. Chem.* **53**, 2998 (2010).
23. J. L. McKimm-Breschkin, *Antiviral Res.* **47**, 1 (2000).
24. M. Tisdale, *Rev. Med. Virol.* **10**, 45 (2000).
25. C. I. Thompson, W. S. Barclay, M. C. Zambon, *J. Antimicrob. Chemother.* **53**, 759 (2004).
26. E. G. Brown, H. Liu, L. C. Kit, S. Baird, M. Nesrallah, *Proc. Natl. Acad. Sci. U.S.A.* **98**, 6883 (2001).
27. M. D. Winn *et al.*, *Acta Crystallogr. D* **67**, 235 (2011).
28. M. Chandler *et al.*, *J. Chem. Soc.-Perkin Trans. 1*, 1173 (1995).
29. A. G. Santana, C. G. Francisco, E. Suarez, C. C. Gonzalez, *J. Org. Chem.* **75**, 5371 (2010).
30. K. Feichtinger, C. Zapf, H. L. Sings, M. Goodman, *J. Org. Chem.* **63**, 3804 (1998).
31. A. G. Watts, S. G. Withers, *Can. J. Chem.* **82**, 1581 (2004).
32. A. G. Watts, P. Oppezzo, S. G. Withers, P. M. Alzari, A. Buschiazzi, *J. Biol. Chem.* **281**, 4149 (2006).
33. R. Leatherbarrow, *Erithacus Software Ltd., 4th Edition, Staines, UK*, (1990).
34. J. L. McKimm-Breschkin, C. Rootes, P. G. Mohr, S. Barrett, V. A. Streltsov, *J. Antimicrob. Chemother.* **67**, 1874 (2012).
35. W. G. Laver, P. M. Colman, R. G. Webster, V. S. Hinshaw, G. M. Air, *Virology* **137**, 314 (1984).
36. T. M. McPhillips *et al.*, *J. Synchrotron. Radiat.* **9**, 401 (2002).
37. Z. Otwinowski, W. Minor, *Methods Enzymol.*, **276**, 307 (1997).
38. P. A. Karplus, K. Diederichs, *Science* **336**, 1030 (2012).
39. A. J. McCoy *et al.*, *J. Appl. Crystallogr.* **40**, 658 (2007).
40. G. N. Murshudov, A. A. Vagin, E. J. Dodson, *Acta Crystallogr.* **53**, 240 (1997).
41. D. E. McRee, *J. Struct. Biol.* **125**, 156 (1999).
42. D. E. McRee, J. Badger, MIFit Manual © Rigaku, (2003-6).
43. A. T. Brünger, *Nature* **355**, 472 (1992).
44. The PyMOL Molecular Graphics System, Version 1.5.0.3 Schrödinger, LLC
45. A. C. Hurt *et al.*, *Antimicrob. Agents Chemother.* **50**, 1872 (2006).
46. A. J. Oakley *et al.*, *J. Med. Chem.* **53**, 6421 (2010).
47. A. S. Monto *et al.*, *Antimicrob. Agents Chemother.* **50**, 2395 (2006).

Acknowledgments: We thank the Canadian Institutes for Health Research, the Pfizer CDRD Innovation Fund, the Canadian Foundation for Innovation and the BC Knowledge Development fund for support of this work. SGW is supported by a Tier 1 Canada Research Chair. JHK was supported by fellowships from the Korea Research Foundation (KRF-2005-214-C00215) and the Michael Smith Foundation for Health Research. TW was supported by the Netherlands Organization for Scientific Research (NWO) through a Rubicon fellowship. Parts of this work were funded by Grant G0600514 from the MRC UK to AGW and JMB and Pandemic influenza grant 595625 from the NHMRC Australia to JMB. The authors acknowledge the use of the MX1 beamline at the Australian Synchrotron, Victoria, Australia. Coordinates of the complex have been deposited in the Protein Data Bank with codes 3W09. Author contributions: JHK, SBu, TW and HC synthesized the title compounds, RR, SBu, JHK and TW performed enzyme kinetics, AGW performed labeling studies, JMB, and SBa performed PRA and IC₅₀ studies, VAS and PP performed crystallographic analyses, MN and NB performed animal efficacy studies, MP performed initial virology, RL performed pharmacokinetic studies, SGW conceived the idea and directed synthesis and kinetic studies with input from MP and JMB. SGW and JMB principally wrote the manuscript with input from many.

Fig. 1. Structures of key influenza therapeutics, mechanism of action of DFSAs and X-ray structure of inhibited enzyme. A) Chemical structures of cell surface sialic acids, the neuraminidase transition state, zanamivir (Relenza[®]) and oseltamivir (Tamiflu[®]); B) Mechanism of action of the 2,3-difluorosialic acids (DFSAs); C) X-ray crystallographic structure of the active site of the enzyme trapped as its 3-fluoro(eq)-4-guanidino-sialyl-enzyme intermediate (elimination product is in pale cyan) overlaid with omit (2 σ) electron density map shown as a grey mesh contoured at 1 σ within 1.6 Å of ligands. The electron density extends from the ligand molecule to Y406, suggesting a covalent link between the inhibitor's C-2 atom and the OH of Y406; D). Diagram of interactions (orange dashed lines; distances in Å) with the sialic acid in the covalently inhibited enzyme. The corresponding diagram of interactions for the elimination product is shown in fig. S4.

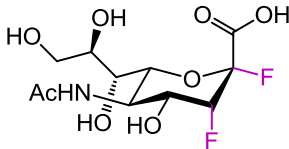
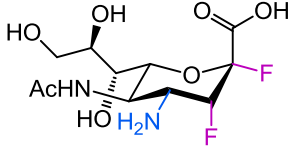
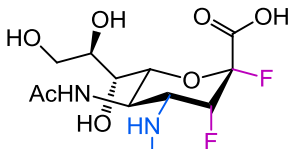
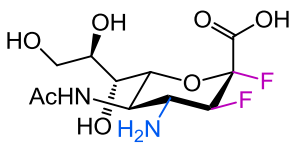
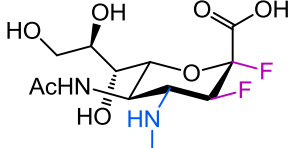
Fig. 2. Efficacy of FaxGuDFSA (3), FeqGuDFSA (5) and zanamivir in treating H3N2 influenza infection in the Balb/c mouse. A) The top graph shows body weight over the 17 day observation period. Animals that lost 20% of initial weight were recorded as non-survivors, as indicated in the survival plot (inset). In a parallel set of animals, viral RNA loads were measured over 7 days by qPCR (bottom graph). In this group, all untreated animals survived only 3 days. B) Dose dependent efficacy of FeqGuDFSA (5) (1-10 mg/kg/d) and zanamivir. FeqGuDFSA (5) was partly (20%) effective at protecting animals at 3 mg/kg/d ((* Mantel Cox p = 0.03), whereas a 10 mg/kg/d dose was 100% effective (dotted line, (***) Mantel Cox p < 0.001).

Table 1. Inactivation and reactivation parameters for difluorosialic acids (DFSAs).

Table 2. IC₅₀ values (nM) in the enzyme inhibition assay for wild type and mutant pairs.

Table 3. IC₅₀ values in the plaque size reduction assay.

Table 1. Inactivation and reactivation parameters for difluorosialic acids (DFSAs). *

Compound	Virus [†]	k_i/K_i ($\text{min}^{-1}\text{mM}^{-1}$)	$t_{1/2}$ (inac) (min)	$t_{1/2}$ (reac) (min)
 DFSA (1)	G70C H1N9	196	N.D. [‡]	< 1 min
 FaxAmDFSAs (2)	Brisbane H1N1	106	2.1	6900
	Brisbane H1N1 H275Y	29	2.5	3450
	California H1N1	95	1.7	6900
	G70C H1N9	74	4.0	2300
	Hong Kong H3N2	140	20.8	>6900
 FaxGuDFSAs (3)	Brisbane H1N1	371	7.4	>6900
	Brisbane H1N1 H275Y	160	9.2	>6900
	California H1N1	93	20.9	>6900
	G70C H1N9	246	6.8	>6900
	Hong Kong H3N2	470	20.2	>6900
 FeqAmDFSAs (4)	Brisbane H1N1	3479	0.9	256
	Brisbane H1N1 H275Y	849	0.2	117
	California H1N1	4422	0.4	46
	G70C H1N9	4332	0.8	49
	Hong Kong H3N2	5662	---	153
 FeqGuDFSAs (5)	Brisbane H1N1	5812	0.3	1380
	Brisbane H1N1 H275Y	2992	0.5	460
	California H1N1	7594	0.9	690
	G70C H1N9	3879	0.5	363
	Hong Kong H3N2	5737	0.8	1380

*Refer to table S4 for full kinetic parameters. [†]Brisbane H1N1 = A/Brisbane/59/07; Brisbane H1N1 H275Y = A/Brisbane/59/07 oseltamivir-resistant; California H1N1 = A/California/07/09; G70C H1N9 = A/NWS/G70C/75; Hong Kong H3N2 = A/HongKong/01/68; [‡]N.D. = Not Determined.

Table 2. IC₅₀ values (nM) in the enzyme inhibition assay for wild type and mutant pairs.

Virus*	Zanamivir	Oseltamivir	DFSA (1)	FaxAm DFSA (2)	FaxGu DFSA (3)	FeqAm DFSA (4)	FeqGu DFSA (5)
B/Perth	8.9	104.4	70	210	54	5.4	4.5
B/Perth D197E	257.5	708.0	170	340	162	16	8
A/Mississippi H1N1	1.9	3.1	80	840	115	45	13
A/Mississippi H1N1 H275Y	2.2	2440	120	2210	217	86	44
A/Fukui H3N2	3.8	1.7	1380	4710	2006	71	25
A/Fukui H3N2 E119V	3.4	260.0	240	2440	998	265	2.4
G70C H1N9	2.7	2.8	1190	2700	66.7	270	140
G70C H1N9 E119G	678.4	2.9	1150	1600	1433	73	17

Red highlights resistance to zanamivir or oseltamivir. The IC₅₀ is the concentration of inhibitor which reduces enzyme activity by 50% compared to the control uninhibited value. Values are the means of duplicate assays. *B/Perth = B/Perth/211/01; B/Perth D197E = B/Perth/211/01 zanamivir and oseltamivir-resistant; A/Mississippi H1N1 = A/Mississippi/3/01; A/Mississippi H1N1 H275Y = A/Mississippi/3/01 oseltamivir-resistant; A/Fukui H3N2 = A/Fukui/45/01; A/Fukui H3N2 E119V = A/Fukui/45/01 oseltamivir-resistant; G70C H1N9 = A/NWS/G70C/75; G70C H1N9 E119G = A/NWS/G70C/75 zanamivir-resistant

Table 3. IC₅₀ values in the plaque size reduction assay.

Virus*	Zanamivir	DFSA (1)	FaxAm DFSA (2)	FaxGu DFSA (3)	FeqAm DFSA (4)	FeqGu DFSA (5)
B/Perth	10 nM	1 µM	100 nM	10-100 nM	10-100 nM	1 nM
A/Mississippi H1N1	≤1 nM	1 µM	100 nM	10 nM	100 nM	1 nM
A/Fukui H3N2	100 nM	100 µM	1 µM	100 nM	1 µM	10 nM
G70C H1N9	1-10 nM	1-10 µM	1 µM	1-10 nM	1 µM	10 nM

The IC₅₀ is the concentration of inhibitor required to reduce plaque size by 50%. Values are the means of duplicate assays. *B/Perth = B/Perth/211/01; A/Mississippi H1N1 = A/Mississippi/3/01; A/Fukui H3N2 = A/Fukui/45/01; G70C H1N9 = A/NWS/ G70C/75.

Supplementary Materials:

Materials and Methods

Figures S1-S8

Tables S1-S3

References (27-47)

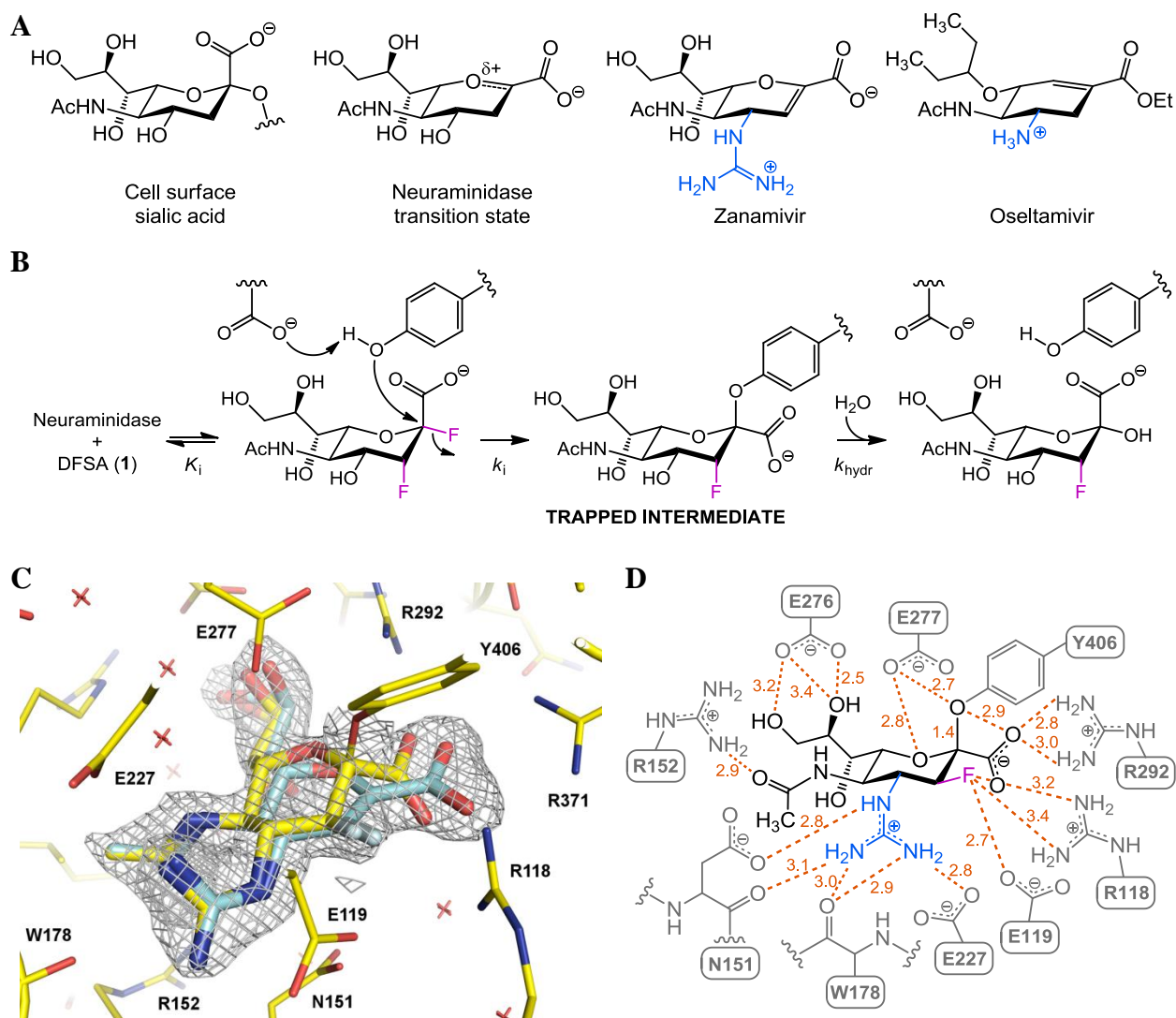


Fig. 1. Structures of key influenza therapeutics, mechanism of action of DFSAs and X-ray structure of inhibited enzyme. A) Chemical structures of cell surface sialic acids, the neuraminidase transition state, zanamivir (Relenza[®]) and oseltamivir (Tamiflu[®]); B) Mechanism of action of the 2,3-difluorosialic acids (DFSAs); C) X-ray crystallographic structure of the active site of the enzyme trapped as its 3-fluoro(eq)-4-guanidino-sialyl-enzyme intermediate (elimination product is in pale cyan) overlaid with omit (27) electron density map shown as a grey mesh contoured at 1σ within 1.6 Å of ligands. The electron density extends from the ligand molecule to Y406, suggesting a covalent link between the inhibitor's C-2 atom and the OH of Y406; D). Diagram of interactions (orange dashed lines; distances in Å) with the sialic acid in the covalently inhibited enzyme. The corresponding diagram of interactions for the elimination product is shown in fig. S4.

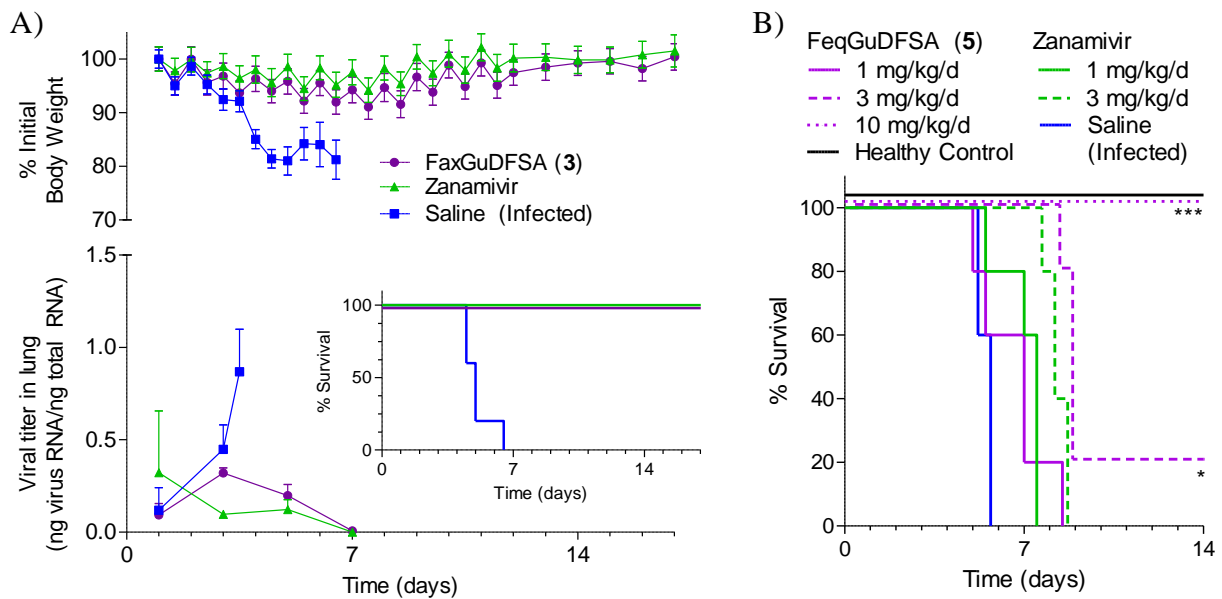


Fig. 2. Efficacy of FaxGuDFSA (3), FeqGuDFSA (5) and zanamivir in treating H3N2 influenza infection in the Balb/c mouse. A) The top graph shows body weight over the 17 day observation period. Animals that lost 20% of initial weight were recorded as non-survivors, as indicated in the survival plot (inset). In a parallel set of animals, viral RNA loads were measured over 7 days by qPCR (bottom graph). In this group, all untreated animals survived only 3 days. B) Dose dependent efficacy of FeqGuDFSA (5) (1-10 mg/kg/d) and zanamivir. FeqGuDFSA (5) was partly (20%) effective at protecting animals at 3 mg/kg/d (** Mantel Cox $p = 0.03$), whereas a 10 mg/kg/d dose was 100% effective (dotted line, (***) Mantel Cox $p < 0.001$).